Effects of strain rate and bond preparation for dissimilar materials in energy dispersive applications

Tom Commins[*], and *Clive R* Siviour

Department of Engineering Science, University of Oxford, Parks Road, Oxford, OX1 3PJ, UK

Abstract. Composite materials, typically consisting of two or more dissimilar materials adhered together in layers, are frequently used for energy absorption applications. The interface and material characteristics strongly influence the global energy absorptive capability of the composite. This research focuses on ceramic-polymer interfaces and, in particular, links between the properties of the composite, the interface and the separate materials. After characterisation of the materials, the effects of impact speed and bond condition were considered for a polymer-ceramic bond in a three-point bend configuration. Specimens were loaded in a screw-driven machine at 0.05 mm s^{-1} and through projectile impact at speeds of approximately 50 m s^{-1}. Screw-driven experiments were performed at ambient and sub ambient conditions, with the temperature chosen to simulate the expected polymer performance in the gas gun experiment, making use of the equivalence of rate and temperature for polymers.

1 Introduction

The ideal material for body armour for ballistic protection would have very high hardness, to fragment or blunt any incoming projectiles, sufficient toughness and ductility to absorb the incident kinetic energy and low enough weight to allow suitable mobility. Materials such as Kevlar are suitable for low energy or relatively soft projectiles; however, for higher energy projectiles, no single material exists. Therefore, composite armour comprising of two dissimilar materials is used [1, 2]. Composite armour consists of a hard ceramic strike face with a ductile backing, typically a polymer or metal. Broadly, this backing layer is present for energy absorption and to limit ceramic fragmentation [3, 4, 5]. The interaction between the two materials strongly influences the global armour performance. Despite this, however, to the authors' knowledge, there has been no methodical fundamental study into the influence of the interface on the global armour response. Therefore, to address this, a fundamental approach to this problem has been proposed where model armours are loaded in simple geometries and the effect of the bond condition can be determined.

2 Overview

The effects of surface preparation and strain rate on energy absorption were investigated for composite polymer-ceramic specimens, Fig. 1, in 3 point bend. To begin, the unsupported ceramic was characterised to determine the influence of the polymer support. Specimens were then loaded under 3 point bend at quasi-static loading on a screw driven compression machine and at high rate using a gas gun.

[*] Corresponding author: thomas.commins@magd.ox.ac.uk
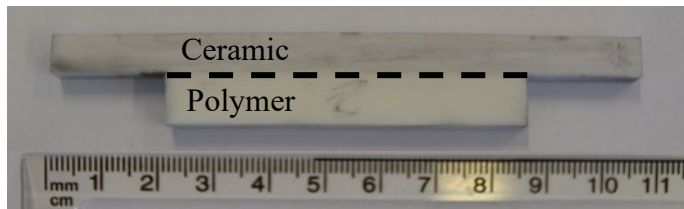
Fig. 1. Typical composite 3 point bend specimen. The central load was applied on the ceramic side and the specimen was painted with a fine speckle pattern for digital image correlation (DIC) analysis.
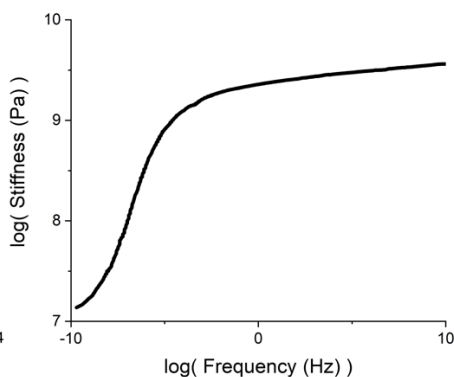
3 Material Characterisation

To determine the influence of the polymer and interfacial behaviour on the composite response, the stiffness and breaking stress of the unbacked ceramics was first measured. Six alumina specimens of dimensions approximately $5 \times 8 \times 100$ mm were loaded in three-point bend, with a span of 80 mm, until failure. From this, the ranges of stiffness and breaking stress were calculated. shows the force – displacement curves measured during these experiments for 6 separate specimens. To account for small changes in specimen dimensions, the force is normalised by the second moment of area of each beam. It is observed that there is a consistent stiffness and a small range of failure loads. The breaking stress can be calculated and fitted to a Weibull distribution [6], which was found to have a Weibull modulus of approximately 17.

For the polymer, polyurethane was tested using a relaxation test in a Dynamic Mechanical Analysis (DMA) machine (TA Q800). A rectangular specimen of dimensions $50 \times 12 \times 2.68$ mm were loaded to 0.1 % strain in 3 point bend and held at this displacement for 10 minutes whilst the force was measured; the specimen was allowed to recover, unloaded, for a further 20 minutes. This was repeated at a range of temperatures from -90 °C to 70 °C in 5 °C intervals. A mastercurve of the polymer's stiffness as a function of frequency can be calculated using time-temperature superposition [7, 8], and is shown in Fig. 3.
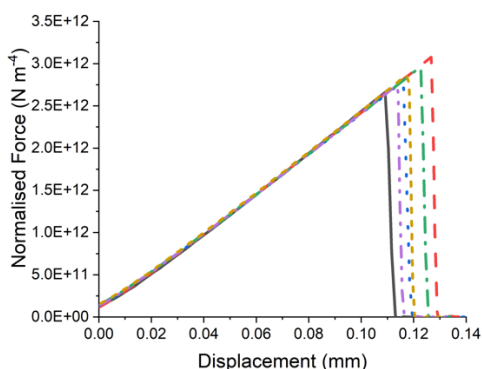
Fig. 2. Normalised Force vs displacement for ceramic specimens in bending. The force was normalised by the second moment of area of each specimen.

Fig. 3. Mastercurve of storage modulus with frequency for polyurethane at room temperature found using DMA.

4 Low rate 3-point bend

After characterisation of the materials, composite beam bend specimens were made. The ceramic strips were first cleaned, and tested in a number of conditions: unsupported ceramic; ceramic with polymer bonded at room temperature, with and without the ceramic surface roughened before bonding; and (unroughened) at -44 °C. This temperature was chosen to simulate the stiffness of the polymer at the microsecond time scales of importance at high strain rate utilising the principle of time-temperature superposition [8]. After degassing and once fully cured, specimens were machined to create a level surface. Finally, a speckle pattern was created using an airbrush to allow Digital Image Correlation (DIC) analysis using MatchID software. From DIC, the correlation map can be used to determine the failure mode;

- *Through Thickness Failure*: If the ceramic fails before the interface, the specimen will fail and break in two, Fig. 4. (a). From DIC analysis, Fig. 5 (a), the correlation map can be used to determine the approximate crack location: if a crack splits the DIC subsets, there is poor correlation. In this case, a through thickness crack is observed splitting the composite specimen and no interfacial failure is seen.

- *Interfacial Failure*: If the interface fails before the ceramic, then an L-shaped crack is formed, initially propagating along the interface and then through the ceramic, creating the failure in Fig. 4 (b). This is confirmed in Fig. 5 (b) where, using the DIC correlation coefficient, a crack is observed to initially propagate along the ceramic-polymer interface before the ceramic has failed. In this situation, the ceramic has effectively lost the support of the polymer in bending.

(a) (b)
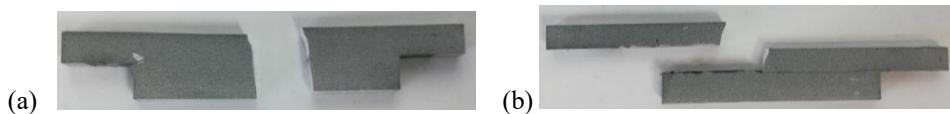
Fig. 4. Failure modes – (a) through thickness and (b) early interface failure


(a) (b)
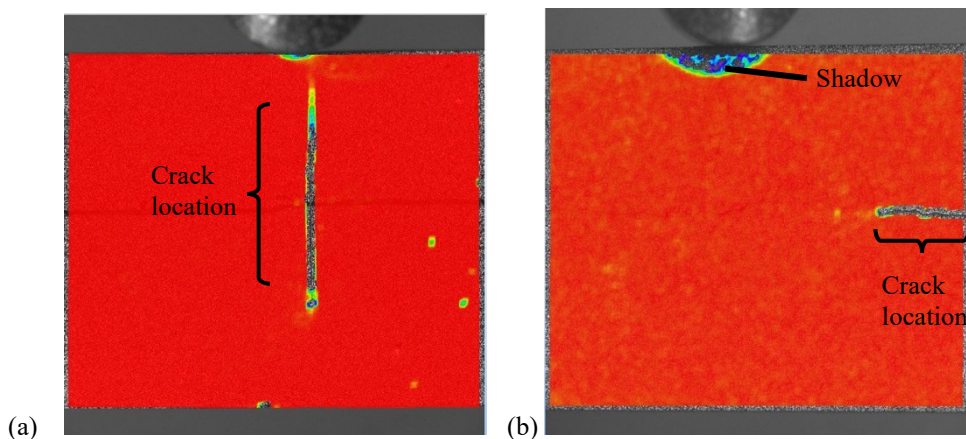
Fig. 5. Map of the DIC correlation coefficient for two specimens displaying the early stages of (a) through thickness and (b) interfacial failure. Cracking interferes with the DIC correlation, allowing crack evolution to be observed. In both cases the influence of the indenter's shadow causes poor correlation at the point of contact.

4.1 Breaking Stress

Fig. 6 shows the breaking stress for all the conditions tested, calculated from simple beam theory at the centre of the ceramic. When the polymer remains bonded to the ceramic and the failure stress of the composite increased by up to 25 % compared to the unbacked ceramic. When the interface fails before the ceramic, the ceramic has lost the backing of the polymer and the breaking stress is similar to that of the unbacked ceramic.

Therefore, at low rate, the composite response is highly dependent upon the interfacial behaviour. In these particular cases, the applied roughening modifications have acted to lower the strength of the interface compared to the unmodified surface. Further, reducing the temperature, and thereby stiffening the polymer, appears to make it more favourable for the crack to propagate along the interface, leading to reduced failure strength of the composite.
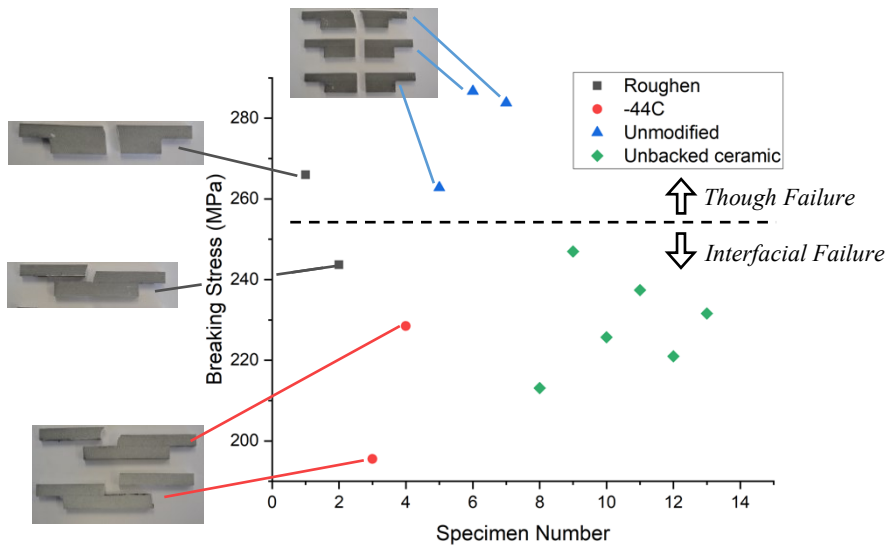
Fig. 6. Ceramic breaking stress calculated from simple beam theory for different surface preparations. Compared to the unbacked ceramic specimens (green diamond ◆), there is a clear increase in breaking stress as long as the polymer stays adhered to the ceramic.

5 Impact 3-point bend

Specimens were then tested in impact using a gas gun. Specimens were manufactured identically to those used for quasi-static experiments and were impacted at a range of speeds from 30 to 50 m s^{-1}. DIC was again used to measure specimen deformation, this time from high-speed images captured at 100 000 frames per second using a Photron SA-X2 camera. The projectile was a cylinder 20 mm x 8 mm diameter with a 4 mm radius machined cylindrical nose. The speed of the projectile was measured using image tracking and the reduction of kinetic energy calculated. The mass of the projectile was assumed to remain constant throughout impact. Various specimen conditions were used: ceramic alone, ceramic with polymer bonded to the back surface and ceramic with a polymer strip held against, but not bonded to, the back using an elastic band. This allows separation of the influence of interfacial strength from that of the polymer mass.
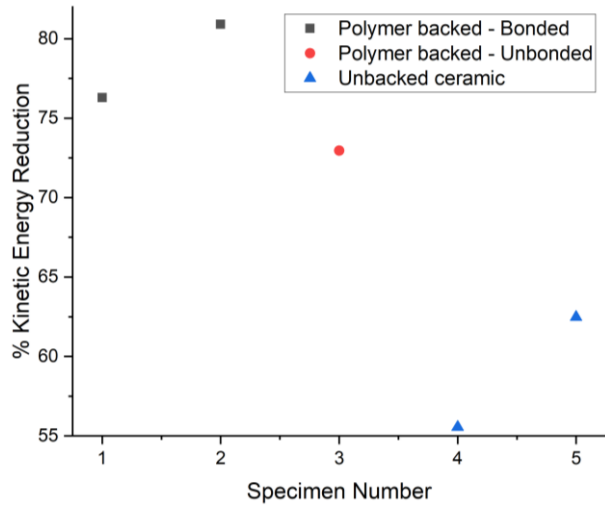
Fig 7. Percentage kinetic energy reduction during impact, calculated using image tracking, comparing across specimen conditions.

The influence of specimen type on kinetic energy reduction is shown in Fig 7. Here, it is seen that the largest improvement in kinetic energy reduction comes from the addition of the polymer mass. However, there are clear performance increases from the addition of interfacial strength. Further, this improvement from the interfacial layer comes with very little increase in mass; therefore, to attain the same armour performance without any interfacial strength would require more mass and increase the areal density.

(a)   (b)   (c)
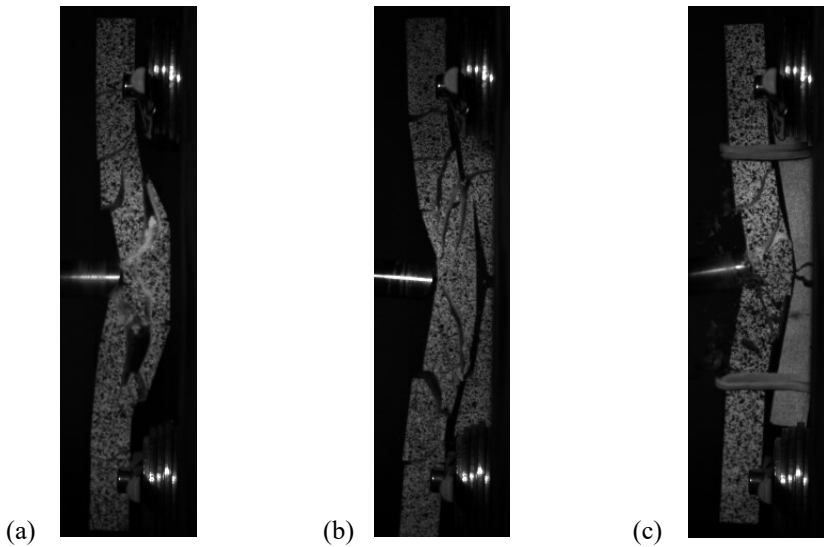
Fig. 8. Failure modes for a) Unbacked ceramic b) polymer backed - Bonded c) polymer backed - Unbonded (polymer backing fixed by an elastic band).

Fig. 8, shows the failure modes for each specimen type. Each specimen fails in a conical shape typical of impact failure in ceramics [2]. For the ceramic only specimen, Fig. 8a, and

the non-bonded specimen, Fig. 8c, there is less fragmentation of the ceramic compared to the bonded specimen, Fig. 8b, which reduces energy absorption. Additionally, in the bonded specimen the fracture of the ceramic occurs closer to the supports and therefore over a larger volume of the ceramic compared to the other two. This has the additional effect that, as well as this additional fracture absorbing energy, the energy is spread over a wider surface.

6 Conclusion

In this study, after characterisation of the materials, the influence of the interface was evaluated at both high and low rates under beam bend. At low rates, the failure stress of the ceramic is heavily dependent on survival of the interface. If the interface survives longer than the ceramic, then it can fully support the ceramic up to the point of failure which increases ceramic strength by approximately 25 %.

At high rates, the influence of the interface was investigated by removing its interfacial strength entirely by attaching the backing polymer with an elastic band and comparing this to a bonded specimen as well as a ceramic only specimen. From this, a clear improvement of the model system comes from the mass of the polymer; however, there is a notable improvement from the adhered interface. Further, the adhered interface increases the area over which the incident energy is spread. To explore this further, additional studies involving a greater number of specimens and bonding surface properties will be performed.

7 Acknowledgements

References

[1] R. Zaera, S. Sanchez-Saez, J. Perez-Castellanos, C. Navarro, Composites: Part A, vol. 31, pp. 823-833, 2000.

[2] P. Hazell, Armour, Chapter 7, CRC Press, 2016.

[3] K. Akella, N. Naik, Journal of the Indian Institute of Science, vol. 95, no. 3, pp. 297-312, 2015.

[4] A. Prakash, J. Rajasankar, N. Anandavalli, M. Verma, N. Iyer, International Journal of Adhesion and Adhesives, vol. 41, pp. 186-197, 2013.

[5] W. Seifert, E. Strassburger, S. Grefen and S. Schaare, Defence Technology, vol. 12, pp. 188-200, 2016.

[6] J. Lemaitre, R. Desmorat, Engineering Damage Mechanics, Chapter 7, Springer, 2005.

[7] M. Oregui, A. de Man, M.F. Woldekidan, Z. Li, R. Dollevoet, Journal of Sound and Vibration, vol. 363, pp. 460-472, 2016.

[8] M. J. Kendall, C. R. Siviour, Polymer, vol. 54, Issue 18, pp. 5058-5063, 2013.